



Published in final edited form as:

J Immunol. 2021 February 01; 206(3): 465–470. doi:10.4049/jimmunol.2001163.

Cutting Edge: Heterogeneity in cell age contributes to functional diversity of natural killer cells

Nicholas M. Adams^{*,1}, Carlos Diaz-Salazar^{*,†,1}, Celeste Dang^{*,‡}, Lewis L. Lanier^{§,¶}, Joseph C. Sun^{*,†,‡}

^{*}Immunology Program, Memorial Sloan Kettering Cancer Center, New York, NY 10065, USA

[†]Department of Immunology and Microbial Pathogenesis, Weill Cornell Medical College, New York, NY 10065, USA

[‡]Louis V. Gerstner, Jr. Graduate School of Biomedical Sciences, Memorial Sloan Kettering Cancer Center, New York, NY 10065, USA

[§]Department of Microbiology and Immunology, University of California San Francisco, San Francisco, CA 94143, USA

[¶]Parker Institute for Cancer Immunotherapy, San Francisco, CA 94129, USA

Abstract

Heterogeneity among naïve adaptive lymphocytes determines their individual functions and fate decisions during an immune response. Natural killer (NK) cells are innate lymphocytes capable of generating ‘adaptive’ responses during infectious challenges. However, the factors that govern various NK cell functions are not fully understood. Here, we use a reporter mouse model to permanently ‘time-stamp’ NK cells and type 1 innate lymphoid cells (ILC1s) in order to characterize the dynamics of their homeostatic turnover. We found that the homeostatic turnover of tissue-resident ILC1s is much slower than that of circulating NK cells. NK cell homeostatic turnover is further accelerated without the transcription factor Eomes. Finally, heterogeneity in NK cell age diversifies NK cell function, with ‘older’ NK cells exhibiting more potent IFN- γ production to activating stimuli, and more robust adaptive responses during cytomegalovirus infection. These results provide insight into how the functional response of an NK cell varies over its lifespan.

Introduction

With unparalleled diversity in its receptor repertoire, adaptive lymphocytes are equipped to recognize nearly any encountered antigen (1). Although TCR engagement is the central event in T cell activation, T cell responsiveness is also shaped by complex events and interactions during its lifespan, from its development to its maturation to its maintenance and differentiation in the periphery. For example, CD8⁺ T cell developmental origin, either

Phone number: 646-888-3228; Fax number: 646-422-0452; sunj@mskcc.org.

¹These authors contributed equally

Disclosures

The authors have no financial conflicts of interest.

from liver hematopoietic stem cells (HSCs) in fetal life or bone marrow HSCs in adult life, epigenetically imprints CD8⁺ T cells, which coincides with distinct effector functions and fate decisions during infection (2). Furthermore, after thymic selection, T cells emerge into the periphery as recent thymic emigrants that possess a unique functional profile compared with mature naïve T cells that have experienced post-thymic maturation (3).

Natural killer (NK) cells are innate lymphocytes that specialize in antitumor and antiviral defense, particularly in the clearance of herpesviruses in both mice and humans (4, 5). NK cell functions span the innate-adaptive continuum, from rapid cytokine production (most notably IFN- γ) and cytotoxicity to ‘adaptive’ responses driven by specific receptor-ligand interactions (6). Adaptive NK cell responses are best defined in the context of cytomegalovirus (CMV) infection, which drives NK cell clonal expansion and establishes long-lived memory NK cells in a manner reminiscent of the antiviral response of adaptive lymphocytes (7, 8). In C57BL/6 mice, a subset of NK cells expresses the activating receptor Ly49H, which recognizes the mouse CMV (MCMV) glycoprotein m157 (9, 10), and drives adaptive NK cell responses to MCMV with comparable kinetics, transcriptome, and epigenetic profiles to simultaneously responding CD8⁺ T cells (11).

Many groups have interrogated the effect of diversity in the NK cell receptor repertoire on antiviral NK cell responses (8). The NK cell receptor profile is established early during development, yet other aspects of NK cell heterogeneity that are introduced during their maintenance and turnover in the periphery are poorly understood. Here, we use a reporter mouse model to permanently ‘time-stamp’ and track group 1 innate lymphocytes (NK cells and ILC1s) during their lifespan, and find that circulating NK cells turn over faster than tissue-resident ILC1s. These studies also provide evidence that homeostatic turnover yields extensive heterogeneity in cell age among naïve group 1 innate lymphocytes, and that cell age is a key variable governing NK cell function.

Materials and Methods

Mice

All mice used in this study were bred under specific pathogen-free conditions at Memorial Sloan Kettering Cancer Center, and handled in accordance with the guidelines of the Institutional Animal Care and Use Committee. The following mouse strains, all on the C57BL/6 background, were used in this study: C;129S4-*Rag2^{tm1.1Flv} Il2rg^{tm1.1Flv}/J (Rag2^{-/-} Il2rg^{-/-}), *Nkp46^{CreERT2}* (12), *Rosa26^{dTomato}* (13), *Nkp46^{CreERT2+} Rosa26^{dTomato/tdTomato} (iNkp46^{dTomato})*, *Eomes^{fl/fl}* (14), and *Nkp46^{CreERT2+} Rosa26^{dTomato/tdTomato} Eomes^{fl/fl}*. Experiments were conducted using age- and gender-matched mice in accordance with approved institutional protocols.*

Tamoxifen

To timestamp NK cells, *iNkp46^{dTomato}* mice were administered 1 mg of tamoxifen (Sigma) dissolved in 0.2 ml corn oil (Sigma) by oral gavage.

Virus preparation and infection

MCMV (Smith strain) was serially passaged through BALB/c hosts three times. Stocks were prepared by using a dounce homogenizer to dissociate the salivary glands of infected mice 3 weeks after infection. *Rag2^{-/-} Il2rg^{-/-}* recipients were infected with 7.5×10^2 PFU MCMV stock by i.p. injection on the day after adoptive splenocyte transfer.

Ex vivo stimulation of NK cells

Five hundred thousand splenocytes were cultured for 5 h in RPMI-1640 containing 10% FBS and 1000 IU/ml of human IL-2 (Roche) (media) in the presence of the following stimuli: 20 ng/ml recombinant mouse IL-12 (R&D Systems) plus 10 ng/ml IL-18 (MBL), 10 ng/ml PMA (Sigma) plus 1 μ g/ml ionomycin (Sigma), or 10 μ g/ml of plate-bound anti-mouse antibodies (BioLegend) against NK1.1 (PK136), Ly49H (3D10), Ly49D (4E5), or Nkp46 (29A1.4) coated on 96-well high bind plates (Corning). Brefeldin A (BioLegend) and BD Golgi Stop were added to the media 1 h into the stimulation, and anti-mouse CD107a antibody was added 2 h into the stimulation. Cells were cultured in media alone as a negative control.

Flow cytometry

Fc receptors were blocked with 2.4G2 mAb before staining with surface or intracellular fluorophore-conjugated anti-mouse antibodies (BD Biosciences, eBioscience, BioLegend, Tonbo Biosciences). Intracellular staining for cytokines was performed by first fixing with 2% paraformaldehyde to preserve tdTomato expression, followed by further fixation and permeabilization with the eBioscience Foxp3 Transcription Factor Staining Set (Thermo Fisher). Flow cytometry was performed on an LSR II cytometer (BD Biosciences). Data were analyzed with FlowJo software (Tree Star).

Statistical analysis

For graphs, data are shown as mean \pm S.E.M. Statistical analyses as described in the figure legends. $p < 0.05$ was considered significant. Graphs were produced and statistical analyses were performed using GraphPad Prism.

Results

Modeling NK cell homeostatic turnover in *iNkp46^{tdTomato}* mice reveals heterogeneity in NK cell age

To model NK cell homeostatic turnover, we used a previously developed transgenic mouse expressing the CreERT2 recombinase under control of the *Ncr1* gene on a bacterial artificial chromosome (12), which we intercrossed with mice bearing a *loxP*-flanked STOP cassette preventing transcription of a tdTomato reporter allele in the *Rosa26* locus (13). Administration of tamoxifen to *Nkp46^{CreERT2+} Rosa26^{tdTomato/tdTomato}* mice (abbreviated *iNkp46^{tdTomato}*) was shown to efficiently label immature and mature NK cells in the periphery, but not precursor NK cells in the bone marrow (12). Thus, tdTomato reporter expression permanently ‘time-stamps’ NK cells present upon tamoxifen administration, enabling the longitudinal analysis of this NK cell population as it ‘ages’. *iNkp46^{tdTomato}*

mice gavaged with tamoxifen maximally labeled peripheral blood NK cells with tdTomato (Tom⁺) at day 3 post tamoxifen (PT) (Figure 1A). We observed a progressive decline in Tom⁺ NK cell frequency over time (Figure 1A), indicating their homeostatic turnover, and their replacement by Tom⁻ NK cells derived from bone marrow progenitors to ensure constant niche size. Fitting a one phase decay model estimated the half-life of peripheral blood NK cells at 19.4 days (14.4–29.2 days, 95% confidence interval) (Figure 1A), which is consistent with earlier reports that relied on BrdU labeling (15). Collectively, these data suggest that at any given snapshot in time, the naïve NK cell pool is a mosaic of NK cells with distinct cell ages.

The maturation status of the declining pool of Tom⁺ NK cells remained relatively constant over time, as measured by CD11b, CD27, and KLRG1 (Figure 1B), indicating that NK cell ‘aging’ and terminal maturation are distinct processes. However, the ‘older’ Tom⁺ NK cells displayed a shift in its receptor repertoire, with a greater frequency of NK cells expressing the activating receptors Ly49H and Ly49D and the inhibitory receptor Ly49A (which has no ligand in C57BL/6 mice), and fewer NK cells expressing the inhibitory receptor NKG2A at day 39 PT compared with day 7 PT (Figure 1C). The skewing of the genetically hard-wired Ly49 profile suggests that certain NK cell clones are favored for longevity. Thus, longitudinal analysis of time-stamped NK cells, performed with tamoxifen treatment of *iNkp46^{tdTomato}* mice, enables modeling of NK cell homeostatic turnover and reveals heterogeneity among naïve NK cells on the basis of cell age.

Eomes is required for the homeostasis, but not terminal maturation, of peripheral NK cells

The identity, maturation, and function of conventional NK cells is determined by a plethora of transcription factors, including Eomesodermin (Eomes) and T-box expressed in T cells (Tbet) (16, 17), that work cooperatively during NK cell development to yield productive NK cells. We leveraged our newly developed *iNkp46^{tdTomato}* time-stamp strategy to dissect the effect of Eomes on mature NK cell homeostatic turnover, independent of its critical role in NK cell development in the bone marrow. We crossed *iNkp46^{tdTomato}* mice with *Eomes^{fl/fl}* mice (*Eomes*^{-/-}) and longitudinally assessed the frequency and maturation status of Eomes-deficient Tom⁺ NK cells after tamoxifen administration. We first confirmed the efficient reduction of Eomes protein in *Eomes*^{-/-} NK cells at day 3 PT (Figure 2A). Acute depletion of Eomes in peripheral NK cells resulted in a faster decline in Tom⁺ NK cells over time, with a shorter half-life (8.8 days, 95% confidence interval = 6.6–12.9 days) than Eomes-sufficient Tom⁺ NK cells from *Eomes*^{WT} control mice (Figure 2B). A recent study similarly implicated Eomes in mature NK cell homeostasis, although the authors show a stage-specific requirement for Eomes in NK cell terminal maturation (18). However, we observed that similar to *Eomes*^{WT} Tom⁺ NK cells, the terminal maturation of *Eomes*^{-/-} NK cells (as measured by CD11b, CD27, and KLRG1) remained relatively constant over time (Figures 2C and 2D). Thus, NK cell homeostasis, but not terminal maturation, is dependent on sustained Eomes expression.

Homeostatic turnover of tissue-resident ILC1s is slower than circulating NK cells

Group 1 innate lymphocytes are a spatially, phenotypically, and functionally heterogeneous family of cells that share the capacity for IFN- γ production and a developmental

dependence on T-bet (19). Group 1 innate lymphocytes are composed of circulating, cytotoxic NK cells and helper-like ILC1s that maintain long-term tissue residency (20). We thus sought to model group 1 innate lymphocyte homeostatic turnover in various tissues, an effort facilitated by the fact that all ILC1s also express NKp46 and are labeled with tdTomato in tamoxifen-treated *iNkp46^{tdTomato}* mice (12). To do so, we harvested spleen, liver, and lungs from cohorts of tamoxifen-induced *iNkp46^{tdTomato}* mice at various time points PT.

Consistent with their status as circulating cells, NK cells displayed comparable homeostatic turnover across all anatomical sites analyzed (Figure 3A). However, despite comparable initial tdTomato labeling of NK cells and ILC1s in the liver (the primary tissue site of murine ILC1s), the Tom⁺ ILC1 frequency decayed more slowly compared with NK cells (Figures 3B and 3C). A similar trend was observed in the lung when NK cells and ILC1s were normalized to account for different initial tdTomato labeling efficiencies (Figure 3D). In both the liver and lung, the Tom⁺ ILC1 frequency ranged from ~4.5- to 7.4-times greater than that of NK cells (Figures 3C and 3D), indicating that ILC1 homeostatic turnover is ~2-3-fold slower than NK cells. Given that ILCs are thought to seed tissues during fetal and perinatal life, and be maintained in adulthood predominantly through local self-renewal with a limited contribution from circulating precursors (21), the greater self-renewal or longer half-life of ILC1s may adapt them for longevity in tissue. These findings collectively indicate that ILC1 homeostatic turnover also introduces heterogeneity in cell age among naïve ILC1s but at a slower rate than NK cells, perhaps as a consequence of or to meet the unique demands of tissue residency.

NK cell effector function and adaptive responses vary with cell age

Having established that homeostatic turnover introduces heterogeneity in cell age among naïve NK cells, we sought to investigate whether NK cell effector function varies over its lifespan. To do so, we evaluated the response of relatively ‘old’ (Tom⁺) versus ‘young’ (Tom⁻) NK cells from tamoxifen-treated *iNkp46^{tdTomato}* mice at day 29–39 PT during *ex vivo* stimulation and *in vivo* challenge with MCMV infection. In response to diverse activating stimuli, a greater percentage of old Tom⁺ NK cells produced IFN- γ (Figure 4A). However, Tom⁺ and Tom⁻ NK cells degranulated comparably when their activating receptors were ligated (Figure 4B), suggesting that cytokine production but not cytotoxic function is dependent on NK cell age.

In addition to their traditional innate-like functions above, NK cells can mount ‘adaptive’ responses, particularly against MCMV infection, characterized by robust clonal proliferation and establishment of immunological memory driven by a specific activating receptor-ligand interaction (Ly49H-m157) (7). To definitively track the fate of existing NK cells during their antiviral response, we adoptively transferred splenocytes, containing Tom⁺ and Tom⁻ NK cells, into *Rag2^{-/-} Il2rg^{-/-}* recipients, which lack endogenous NK cells. Compared with the pre-infection frequency of Tom⁺ NK cells within transferred Ly49H⁺ NK cells, older Tom⁺ NK cells progressively outcompeted their younger Tom⁻ counterparts during both expansion (day 7 post infection) and memory formation (day 29 post infection) (Figures 4C and 4D). In contrast, older Tom⁺ Ly49H⁻ NK cells did not exhibit any selective advantage

over younger Tom⁻ cells over the course of MCMV infection (Figure 4D), suggesting that the greater fitness of ‘aged’ NK cells is required in the setting of robust antigen-driven proliferation, but not modest cytokine-driven bystander proliferation. Compared with Tom⁻ NK cells, Tom⁺ NK cells were slightly more mature following MCMV-driven expansion, but despite their differential memory formation, Tom⁺ and Tom⁻ Ly49H⁺ NK cells similarly underwent terminal maturation (Figure 4E). Collectively, these data reveal that the intrinsic age of an NK cell regulates its functional response to stimulation and viral challenge.

Discussion

Our study reveals that the peripheral compartment of naïve NK cells is comprised of layers of differentially ‘aged’ NK cells, generated by continuous waves of homeostatic turnover and repopulation from bone marrow progenitors. Longer-lived naïve NK cells mount more robust antigen-specific proliferation and memory formation to MCMV. Collectively our data show that NK cell antiviral function is heterogeneous, with NK cell age at the time of viral challenge being a key determinant of its functional response. We also observed that the aging of the NK cell pool coincides with a marked shift in its receptor repertoire, suggesting that some NK cell clones are favored for longevity during homeostasis. Our model does not exclude the possibility that enrichment for these clones, which may be programmed for enhanced functionality, contributes to the results obtained from ‘old’ NK cells.

Interestingly, homeostatic turnover is not constant among all group 1 innate lymphocytes, but rather ILC1s are maintained longer than NK cells across several tissues. ILCs are thought to self-renew with limited repopulation from hematogenous progenitors (20), so it is tempting to speculate that the delayed kinetics of ILC1 homeostatic turnover represents an adaptation to tissue residency, and is integral for the maintenance of barrier immunity over host lifespan. Future work is required to unravel the cell-intrinsic and cell-extrinsic mechanisms that support the self-renewal and longevity of ILC1s in tissue. For instance, is the prolonged lifespan of ILC1s regulated transcriptionally by factors that also program them for tissue residency? And what is the contribution of the distinct microenvironment that ILC1s are exposed to in the tissue parenchyma?

In summary, our work highlights how homeostatic turnover of group 1 ILCs controls the maintenance and function of these cells, from the longevity of tissue-resident ILCs to the antiviral responses of NK cells. Because NK cells are emerging as a promising cell therapy for cancer and infectious disease, it will be important to investigate the dependency of human NK cell responses on their intrinsic age, and to appropriately consider NK cell age in adoptive cell therapies.

Acknowledgments

We thank members of the Sun Lab for experimental assistance and helpful discussions. Graphical abstract was created with BioRender.

N.M.A. was supported by a Medical Scientist Training Program grant from the NIH National Institute of General Medical Sciences (T32GM007739 to the Weill Cornell/Rockefeller/Sloan Kettering Tri-Institutional MD-PhD Program) and by an F30 Predoctoral Fellowship from the NIH National Institute of Allergy and Infectious Diseases (F30 AI136239). C.D.S. was supported by a Fulbright Fellowship from the Commission for Cultural, Educational and Scientific Exchange between the United States of America and Spain. L.L.L. is supported by the Parker

Institute for Cancer Immunotherapy and NIH grant AI068129. J.C.S. is supported by the Ludwig Center for Cancer Immunotherapy, the American Cancer Society, the Burroughs Wellcome Fund, and NIH grants AI100874, AI130043, and P30CA008748.

Abbreviations used in this article:

Eomes	Eomesodermin
ILC	innate lymphoid cell
KLRG1	killer cell lectin-like receptor G1
MCMV	mouse CMV
PI	post infection
PT	post tamoxifen
WT	wild-type

References

1. Goldrath AW, and Bevan MJ. 1999. Selecting and maintaining a diverse T-cell repertoire. *Nature* 402: 255–262. [PubMed: 10580495]
2. Smith NL, Patel RK, Reynaldi A, Grenier JK, Wang J, Watson NB, Nzingha K, Yee Mon KJ, Peng SA, Grimson A, Davenport MP, and Rudd BD. 2018. Developmental Origin Governs CD8(+) T Cell Fate Decisions during Infection. *Cell* 174: 117–130. [PubMed: 29909981]
3. Fink PJ, and Hendricks DW. 2011. Post-thymic maturation: young T cells assert their individuality. *Nat. Rev. Immunol* 11: 544–549. [PubMed: 21779032]
4. Biron CA, Byron KS, and Sullivan JL. 1989. Severe herpesvirus infections in an adolescent without natural killer cells. *N. Engl. J. Med* 320: 1731–1735. [PubMed: 2543925]
5. Bukowski JF, Warner JF, Dennert G, and Welsh RM. 1985. Adoptive transfer studies demonstrating the antiviral effect of natural killer cells in vivo. *J. Exp. Med* 161: 40–52. [PubMed: 2981954]
6. Sun JC, and Lanier LL. 2011. NK cell development, homeostasis and function: parallels with CD8⁺ T cells. *Nat. Rev. Immunol* 11: 645–657. [PubMed: 21869816]
7. Sun JC, Beilke JN, and Lanier LL. 2009. Adaptive immune features of natural killer cells. *Nature* 457: 557–561. [PubMed: 19136945]
8. Adams NM, Grassmann S, and Sun JC. 2020. Clonal expansion of innate and adaptive lymphocytes. *Nat Rev Immunol* 20: 694–707. [PubMed: 32424244]
9. Arase H, Mocarski ES, Campbell AE, Hill AB, and Lanier LL. 2002. Direct recognition of cytomegalovirus by activating and inhibitory NK cell receptors. *Science* 296: 1323–1326. [PubMed: 11950999]
10. Smith HR, Heusel JW, Mehta IK, Kim S, Dorner BG, Naidenko OV, Iizuka K, Furukawa H, Beckman DL, Pingel JT, Scalzo AA, Fremont DH, and Yokoyama WM. 2002. Recognition of a virus-encoded ligand by a natural killer cell activation receptor. *Proc. Natl. Acad. Sci. USA* 99: 8826–8831. [PubMed: 12060703]
11. Lau CM, Adams NM, Geary CD, Weizman OE, Rapp M, Pritykin Y, Leslie CS, and Sun JC. 2018. Epigenetic control of innate and adaptive immune memory. *Nat. Immunol* 19: 963–972. [PubMed: 30082830]
12. Nabekura T, and Lanier LL. 2016. Tracking the fate of antigen-specific versus cytokine-activated natural killer cells after cytomegalovirus infection. *J. Exp. Med* 213: 2745–2758. [PubMed: 27810928]
13. Madisen L, Zwingman TA, Sunkin SM, Oh SW, Zariwala HA, Gu H, Ng LL, Palmiter RD, Hawrylycz MJ, Jones AR, Lein ES, and Zeng H. 2010. A robust and high-throughput Cre

- reporting and characterization system for the whole mouse brain. *Nat Neurosci* 13: 133–140. [PubMed: 20023653]
14. Zhu Y, Ju S, Chen E, Dai S, Li C, Morel P, Liu L, Zhang X, and Lu B. 2010. T-bet and eomesodermin are required for T cell-mediated antitumor immune responses. *J Immunol* 185: 3174–3183. [PubMed: 20713880]
 15. Jamieson AM, Isnard P, Dorfman JR, Coles MC, and Raulet DH. 2004. Turnover and proliferation of NK cells in steady state and lymphopenic conditions. *J Immunol* 172: 864–870. [PubMed: 14707057]
 16. Dausy C, Faure F, Mayol K, Viel S, Gasteiger G, Charrier E, Bienvenu J, Henry T, Debien E, Hasan UA, Marvel J, Yoh K, Takahashi S, Prinz I, de Bernard S, Buffat L, and Walzer T. 2014. T-bet and Eomes instruct the development of two distinct natural killer cell lineages in the liver and in the bone marrow. *J Exp Med* 211: 563–577. [PubMed: 24516120]
 17. Gordon SM, Chaix J, Rupp LJ, Wu J, Madera S, Sun JC, Lindsten T, and Reiner SL. 2012. The transcription factors T-bet and Eomes control key checkpoints of natural killer cell maturation. *Immunity* 36: 55–67. [PubMed: 22261438]
 18. Wagner JA, Wong P, Schappe T, Berrien-Elliott MM, Cubitt C, Jaeger N, Lee M, Keppel CR, Marin ND, Foltz JA, Marsala L, Neal CC, Sullivan RP, Schneider SE, Keppel MP, Saucier N, Cooper MA, and Fehniger TA. 2020. Stage-Specific Requirement for Eomes in Mature NK Cell Homeostasis and Cytotoxicity. *Cell Rep* 31: 107720. [PubMed: 32492428]
 19. Adams NM, and Sun JC. 2018. Spatial and temporal coordination of antiviral responses by group 1 ILCs. *Immunol Rev* 286: 23–36. [PubMed: 30294970]
 20. Gasteiger G, Fan X, Dikiy S, Lee SY, and Rudensky AY. 2015. Tissue residency of innate lymphoid cells in lymphoid and nonlymphoid organs. *Science* 350: 981–985. [PubMed: 26472762]
 21. Kotas ME, and Locksley RM. 2018. Why Innate Lymphoid Cells? *Immunity* 48: 1081–1090. [PubMed: 29924974]

Key points:

- Homeostatic turnover generates heterogeneity in cell age among naïve group 1 ILCs.
- Turnover of tissue-resident ILC1s is slower than that of circulating NK cells.
- Older NK cells mount more robust adaptive responses during CMV infection.

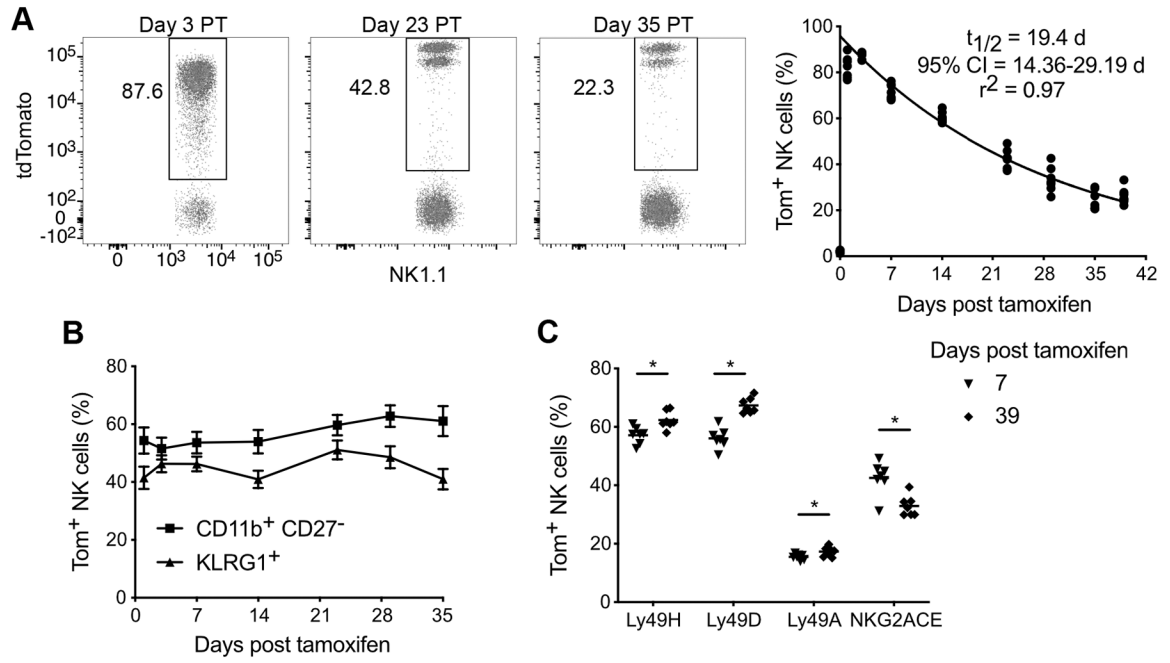


Figure 1. *iNkp46^{tdTomato}* mice are a tool to characterize NK cell homeostatic turnover.

(A) Flow plots illustrating percentage of NK cells (TCR β ⁻ CD3e⁻ NK1.1⁺) expressing tdTomato (Tom⁺) in blood at indicated days post tamoxifen (PT) (left). Data were fitted with one phase decay curve between day 3–39 PT (right). $t_{1/2}$ parameter represents half-life of the best-fit curve, and r^2 indicates the goodness-of-fit of the model to the experimental data.

(B) Percentage of blood Tom⁺ NK cells within the most mature CD11b⁺ CD27⁻ subset or expressing KLRG1 at indicated days PT.

(C) Percentage of blood Tom⁺ NK cells expressing the indicated activating and inhibitory receptors at day 7 PT or day 39 PT. Horizontal bar indicates mean. Groups were compared via a paired, two-tailed t test.

Data are representative of at least 3 independent experiments with 3–7 mice per experiment. Data are presented as the mean \pm S.E.M. * $p < 0.05$.

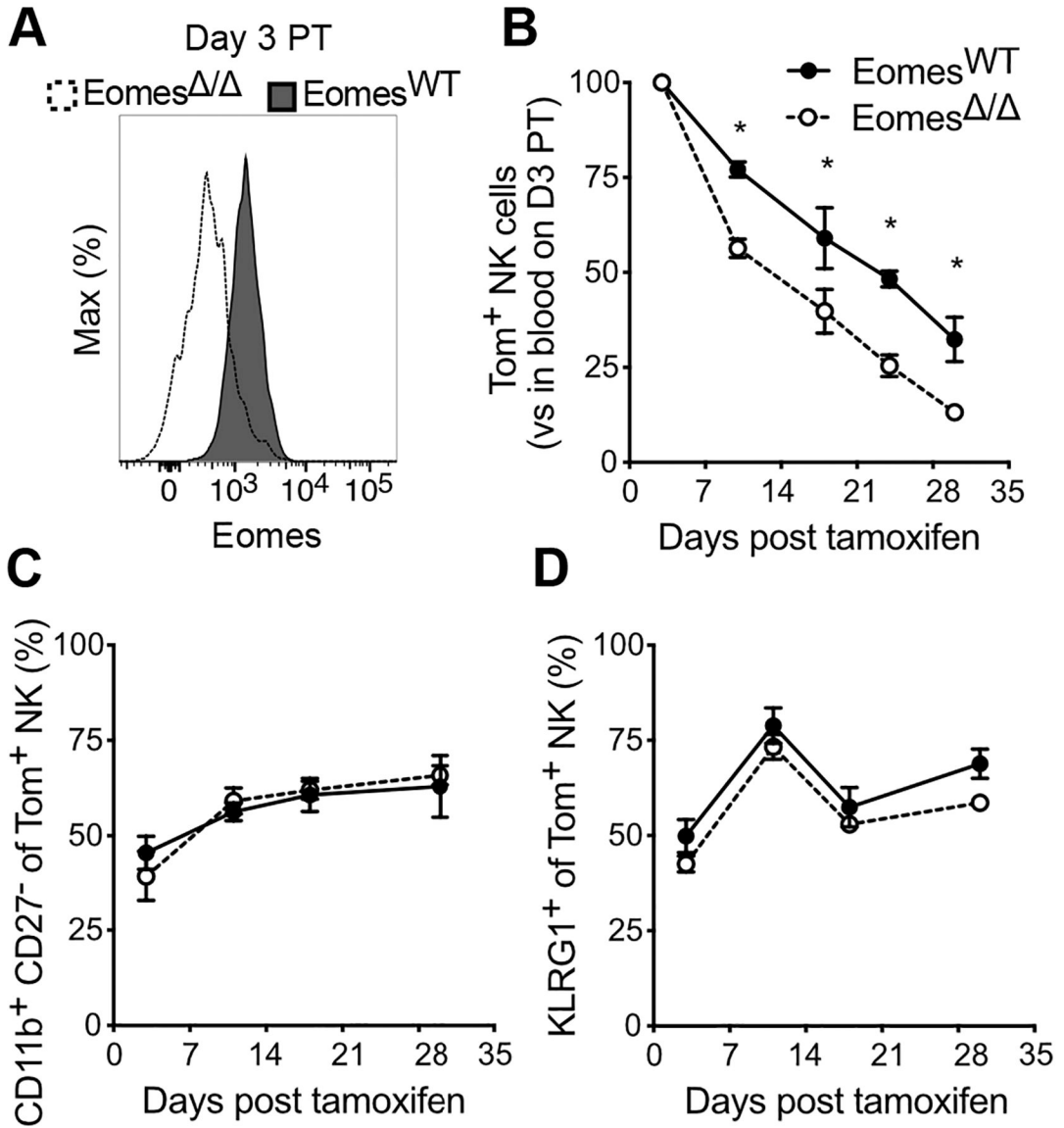


Figure 2. The transcription factor Eomes controls the homeostasis of peripheral NK cells
 (A) Histograms showing Eomes expression in peripheral blood NK cells from *Eomes*^{WT} and *Eomes*^{Δ/Δ} mice at day 3 PT.
 (B) Percentage of Tom⁺ NK cells in blood of *Eomes*^{WT} and *Eomes*^{Δ/Δ} mice at indicated days PT, expressed as a ratio relative to % Tom⁺ blood NK cells in that same mouse at day 3 PT. Data were fitted with one phase decay curve between day 3–30 PT to determine $t_{1/2}$ reported in the text.
 (C and D) Percentage of *Eomes*^{WT} and *Eomes*^{Δ/Δ} Tom⁺ blood NK cells within the most mature CD11b⁺ CD27⁻ subset (C) or expressing KLRG1 (D) at indicated days PT. Data are representative of 3 independent experiments with 2–5 mice per group per experiment. Data are presented as the mean ± S.E.M. *p < 0.05.

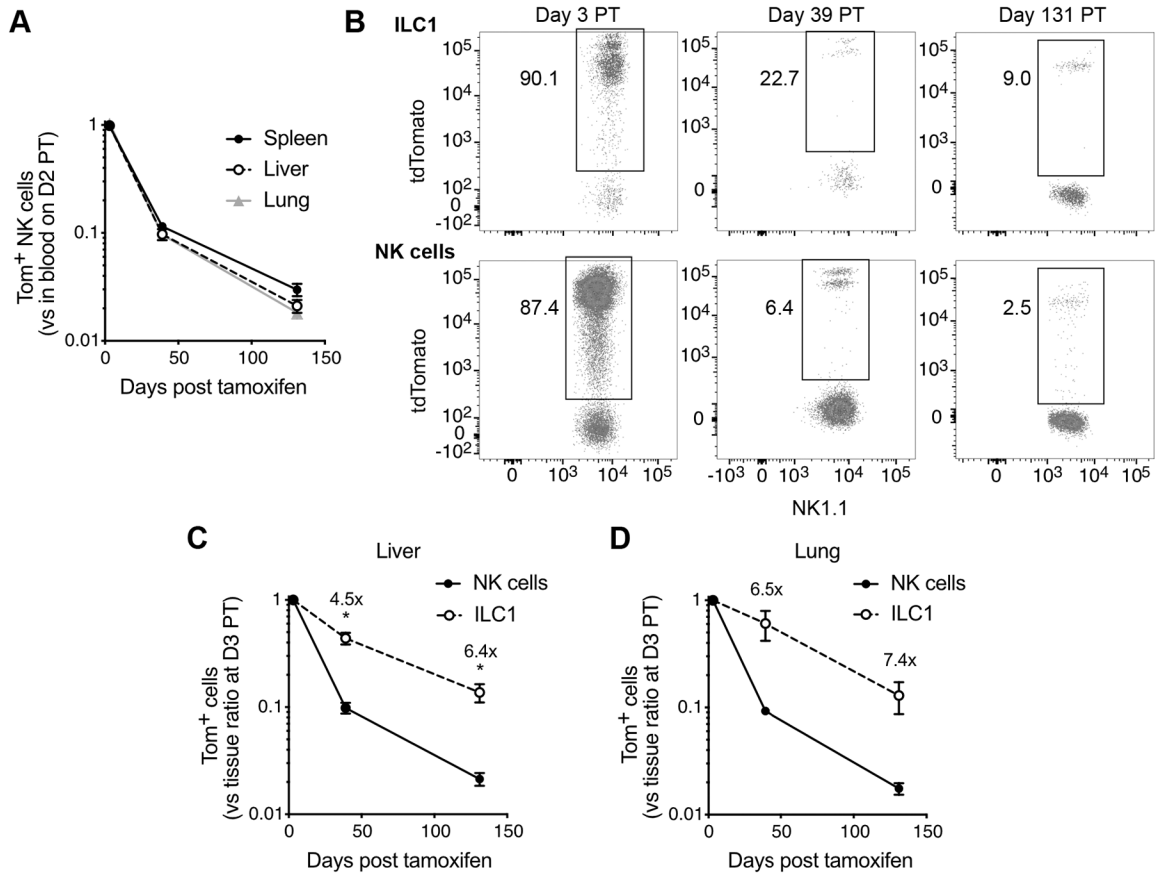


Figure 3. Tissue-resident ILC1s have a longer half-life than circulating NK cells.

(A) Percentage of Tom⁺ NK cells in spleen, liver, and lung at indicated days PT, expressed as a ratio relative to % Tom⁺ blood NK cells in that same mouse at day 2 PT.

(B) Flow plots illustrating percentage of hepatic NK cells (Live Lin⁻ CD45⁺ NK1.1⁺ NKp46⁺ CD49b⁺ CD200r1⁻) and ILC1s (Live Lin⁻ CD45⁺ NK1.1⁺ NKp46⁺ CD49b⁻ CD200r1⁺) expressing tdTomato at indicated days PT. Lin⁻ : TCRβ⁻ CD3ε⁻ F4/80⁻ CD19⁻.

(C) Quantification of percent Tom⁺ NK cells and ILC1s in liver at indicated days PT, expressed relative to % Tom⁺ blood NK cells in that same mouse at day 2 PT and subsequently normalized to the mean of that same ratio at day 3 PT to account for the initial labeling efficiency.

(D) Percentage of Tom⁺ NK cells and ILC1s in lung at indicated days PT, expressed relative to % Tom⁺ blood NK cells in that same mouse at day 2 PT and subsequently normalized to the mean of that same ratio at day 3 PT to account for the initial labeling efficiency.

Data are representative of 2 independent experiments with 3–4 mice per timepoint. Data are presented as the mean ± S.E.M. At each timepoint PT, the frequency of Tom⁺ NK cells and ILC1s were compared via a paired, two-tailed t test. Fold changes indicate the ratio of mean Tom⁺ ILC1 frequency to mean Tom⁺ NK cell frequency at indicated days PT. *p < 0.05.

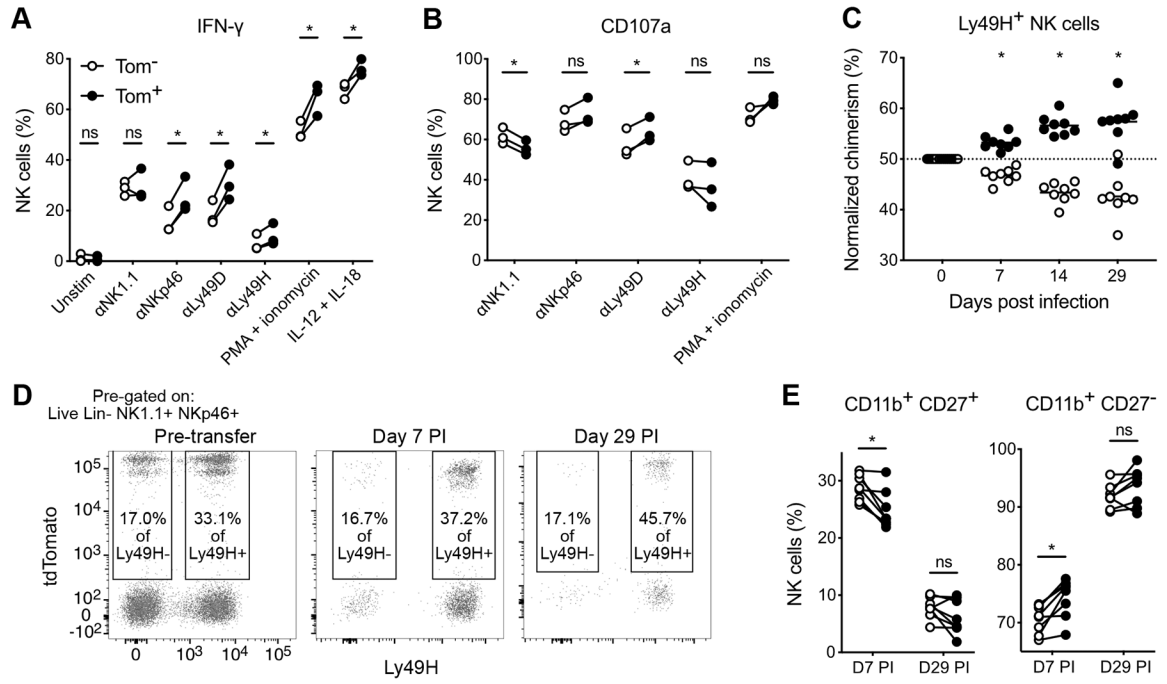


Figure 4. Cell age dictates NK cell effector function and MCMV-driven adaptive responses.

(A and B) Splenocytes harvested at day 29 PT from tamoxifen-treated *iNkp46^{tdTomato}* mice were stimulated *ex vivo*, or maintained in media as a control. Percentage of Tom⁻ or Tom⁺ NK cells producing IFN- γ (A) or degranulating (B) in response to the indicated stimuli. Data are representative of 2 independent experiments with 3–7 mice per experiment. Groups were compared using a paired, two-tailed t test.

(C-E) Splenocytes harvested at day 39 PT from tamoxifen-treated *iNkp46^{tdTomato}* mice were transferred into *Rag2^{-/-} Il2rg^{-/-}* mice 1 day prior to MCMV infection of the recipients. (C) Quantification of relative ratios of Tom⁻ and Tom⁺ Ly49H⁺ NK cells over the duration of MCMV infection, normalized to their pre-infection ratio. Horizontal bar indicates mean. Groups were compared against 50 using a one sample t test. (D) Flow plots of percent Ly49H⁻ and Ly49H⁺ NK cells expressing tdTomato from transferred splenocytes or recipient blood at indicated days post infection (PI). (E) Percentage of Tom⁻ and Tom⁺ Ly49H⁺ NK cells within the CD11b⁺ CD27⁺ or CD11b⁺ CD27⁻ (terminally mature) subsets from peripheral blood at days 7 and 29 PI. Groups were compared using a paired, two-tailed t test. Data are representative of 2 independent experiments with 5–8 mice per experiment. Data are presented as the mean \pm S.E.M. ns, not significant; *p < 0.05.